# *Electronic Supplementary Information (ESI)*

## Materials and instruments

All the other chemicals and reagents were purchased from commercial sources and used as received without further purification. The final products were subjected to vacuum sublimation to further improve purity before photoluminescence (PL) and electroluminescence (EL) properties investigations. $^1$H and $^{13}$C NMR spectra were measured on a Bruker AV 400 or 500 spectrometer in $CDCl_3$ at room temperature. High-resolution mass spectra (HRMS) were recorded on Agilent1290/Bruker maXis impact or on a GCT premier CAB048 mass spectrometer operating in MALDI-TOF mode. Thermal gravimetric analysis (TGA) data were collected from a TG209F1 under nitrogen protection at a heating rate of 20 °C min$^{-1}$. Differential scanning calorimetric (DSC) analysis was performed on a DSC 214 Polymer under dry nitrogen at a heating rate of 10 °C min$^{-1}$. UV-vis absorption spectra were measured on a Shimadzu UV-2600 spectrophotometer. PL spectra were recorded on a Horiba Fluoromax-4 spectrofluorometer. PL quantum yields were measured using a Hamamatsu absolute PL quantum yield spectrometer C11347 Quantaurus QY. Transient PL decay spectra were measured under nitrogen atmosphere (solution) or vacuum (neat film), measured by FLS1000 fluorometer (Edinburgh Instruments). Cyclic voltammograms were recorded in dichloromethane containing 0.1 M tetrabutylammonium hexafluorophosphate with the scan rate of 50 mV s$^{-1}$, using a platinum wire as the auxiliary electrode, a glass carbon disk as the working electrode and $Ag/Ag^+$ as the reference electrode, standardized for the redox couple ferricenium/ferrocene ($Fc/Fc^+$). The redox value of ferrocene for the highest occupied molecular orbital (HOMO) and lowest unoccupied molecular orbital (LUMO) of PytBuCz-XT and PytBuCz-TRZ are about 0.29 and 0.30 eV, respectively. The ground ($S_0$) state and excited singlet ($S_1$) and triplet ($T_1$) states were simulated by performing density functional theory (DFT) and time-dependent density functional theory (TD-DFT) calculations[1] at the level of D3-B3LYP/6-31g(d,p). The energy levels of $S_1$ and $T_1$ states and the corresponding $\Delta E_{ST}$ values were calculated on the basis of the optimized $S_1$ and $T_1$ states. The bond degradation energies (BDEs) were calculated at the level of B3LYP/def2svp.

## Device fabrication and measurement

The glass substrates precoated with a 90-nm layer of indium tin oxide (ITO) with a sheet resistance of

15~20 Ω per square were successively cleaned in ultrasonic bath of acetone, isopropanol, detergent and deionized water, respectively, taking 10 minutes for each step. Then, the substrates were dried in a 70 °C oven. Before the fabrication processes, in order to improve the hole injection ability of ITO, the substrates were treated by $O_2$ plasma for 10 minutes. The vacuum-deposited OLEDs were fabricated under a pressure of $< 5 \times 10^{-4}$ Pa in the Fangsheng OMV-FS380 vacuum deposition system. Organic materials, LiF and Al were deposited at rates of 1~2 A $s^{-1}$, 0.1 A $s^{-1}$ and 5 A $s^{-1}$, respectively. The effective emitting area of the device was 9 $mm^2$, determined by the overlap between anode and cathode. The EL spectra, luminance−voltage−current density and external quantum efficiency were characterized with a dual-channel Keithley 2400 source meter and a PR-670 spectrometer. The external quantum efficiencies were estimated utilizing the normalized EL spectra and the current efficiencies of the devices, assuming that the devices were Lambertian emitters. All the characterizations were conducted at room temperature in ambient conditions without any encapsulation except the lifetime devices, which were encapsulated before the operational lifetime measurement.

**Estimation of photophysical parameters**

The quantum efficiencies and rate constants were determined using the following equations according to the following equations[a)]:

$$\Phi_p = \Phi_F R_p \quad (1)$$

$$\Phi_d = \Phi_F R_d \quad (2)$$

$$k_F = \Phi_p/\tau_p \quad (3)$$

$$\Phi_F = k_F/(k_F + k_{IC}) \quad (4)$$

$$\Phi_p = k_F/(k_F + k_{IC} + k_{ISC}) \quad (5)$$

$$\Phi_{IC} = k_{IC}/(k_F + k_{IC} + k_{ISC}) \quad (6)$$

$$\Phi_{ISC} = k_{ISC}/(k_F + k_{IC} + k_{ISC}) = 1 - \Phi_p - \Phi_{IC} \quad (7)$$

$$\Phi_{RISC} = \Phi_d/\Phi_{ISC} \quad (8)$$

$$k_{RISC} = (k_p k_d \Phi_d)/(k_{ISC}\Phi_p) \quad (9)$$

$$k_p = 1/\tau_p;\ k_d = 1/\tau_d \quad (10)$$

[a)] Abbreviations: $\Phi_{PL}$ = absolute photoluminescence quantum yield; $\tau_p$ and $\tau_d$ = lifetimes calculated from the prompt and delayed fluorescence decay, respectively; $R_p$ and $R_d$ = ratio of prompt component and delayed component and $R_d = 1 - R_p$; $\Phi_p$ and $\Phi_d$ = quantum yields from prompt and delayed components, respectively, determined from the total $\Phi_{PL}$ and the proportion of the integrated area of each component in the transient spectra to the total integrated area; $\Phi_{\mathrm{ISC}}$ = intersystem crossing quantum yield; $k_{\mathrm{F}}$ = fluorescence decay rate; $k_{\mathrm{IC}}$ = internal conversion rate from $S_1$ to $S_0$ states; $k_{\mathrm{ISC}}$ = intersystem crossing rate from $S_1$ to $T_1$ states; $k_{\mathrm{RISC}}$ = rate constant of reverse intersystem crossing.

**Synthesis and characterization**

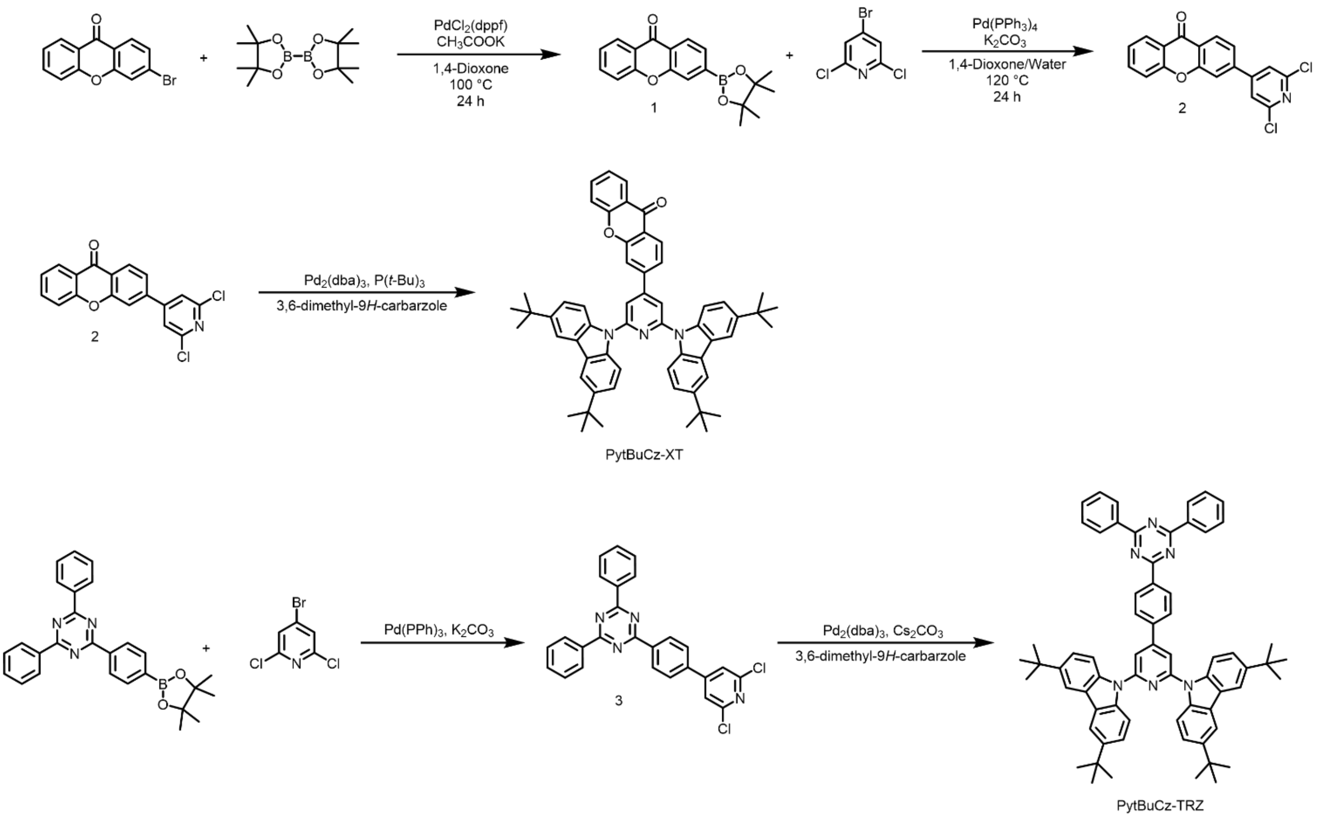

**Scheme S1**. Synthetic routes to new blue TADF molecules.

**3-(2,6-Dichloropyridin-4-yl)-9*H*-xanthen-9-one (2)**: A mixture of 4-bromo-2,6-dichloropyridine (10 mmol, 2.24 g), $K_2CO_3$ (30 mmol, 4.14 g), $Pd(PPh_3)_4$ (1 mmol, 1.15 g) and 3-(4,4,5,5-tetramethyl-1,3,2-dioxaborolan-2-yl)-9*H*-xanthen-9-one (**1**) (10 mmol, 3.22 g) was added to a two-neck flask that was evacuated and backfilled with dry nitrogen. After that, 40 mL 1,4-dioxane and 8 mL pure water were added into the flask. The reaction mixture was refluxed at 120 °C for 24 h and then cooled down to room temperature. The reaction mixture was poured into water and extracted with dichloromethane (20 mL) for three times. The combined organic layers were washed with water and dried over anhydrous $Na_2SO_4$. After filtration and solvent evaporation under reduced pressure, the residue was purified via silica-gel column chromatography using dichloromethane/petroleum ether as eluent. Compound **2** was obtained as white solid in 67.2% yield. $^1$H NMR (500 MHz, $CDCl_3$): $\delta$ (ppm) 8.47 (d, $J$ = 8.3 Hz, 1H), 8.37 (m, 1H), 7.81–7.73 (m, 2H), 7.62–7.51 (m, 4H), 7.47–7.42 (m, 1H). $^{13}$C NMR (125 MHz, DMSO-

*d*$_6$): *δ* 176.72, 156.51, 156.38, 152.13, 151.63 142.03, 135.50, 128.37, 128.60, 127.00, 124.62, 122.71, 122.58, 121.25, 118.20, 116.99.

**2-(4-(2,6-Dichloropyridin-4-yl)phenyl)-4,6-diphenyl-1,3,5-triazine (3)**: The synthetic procedure was analogous to that described for **2**, one of the reactants was purchased from Leyan (4-Bromo-2,6-dichloropyridine (Cat No. 1052959, Leyan, Shanghai, China)) and used without further purification. Compound **3** was obtained as white solid in 89.2% yield. $^1$H NMR (500 MHz, CDCl$_3$): *δ* (ppm) 8.80–8.78 (m, 5H), 7.66–7.56 (m, 11H); $^{13}$C NMR (100 MHz, CDCl$_3$): *δ* 171.88, 153.16, 151.26, 139.35, 138.08, 135.99, 132.78, 129.91, 129.03, 128.75, 128.72, 127.39, 120.94.

**3-(2,6-Bis(3,6-di-*tert*-butyl-9*H*-carbazol-9-yl)pyridin-4-yl)-9*H*-xanthen-9-one (PytBuCz-XT)**: A mixture of compound **2** (8 mmol, 2.73 g), Cs$_2$CO$_3$ (40 mmol, 13 g), P(*t*-Bu)$_3$HBF$_4$ (0.8 mmol, 0.23 g), Pd$_2$(dba)$_3$ (0.8 mmol, 0.73 g) and carbazole (32 mmol, 5.35 g) was added to a two-neck flask that was evacuated and backfilled with dry nitrogen. After that, 40 mL dry 1,4-dioxane and 8 mL pure water were added into the flask. The reaction mixture was refluxed at 110 °C for 24 h and then cooled down to room temperature. The reaction mixture was poured into water and extracted with dichloromethane (20 mL) for three times. The combined organic layers were washed with water and dried over anhydrous Na$_2$SO$_4$. After filtration and solvent evaporation under reduced pressure, the residue was purified via silica-gel column chromatography using dichloromethane/petroleum ether as eluent. Light yellow solid of PytBuCz-XT was obtained in 73.2% yield. $^1$H NMR (500 MHz, CDCl$_3$): *δ* (ppm) 8.52 (d, *J* = 8.2 Hz, 1H), 8.39 (m, 1H), 8.15 (d, *J* = 1.8 Hz, 4H), 8.05 (d, *J* = 8.7 Hz, 4H), 7.89 (d, *J* = 1.5 Hz, 1H), 7.86 (s, 2H), 7.82–7.74 (m, 2H), 7.58–7.56 (m, 1H), 7.50 (m, 4H), 7.46–7.44 (s, 1H), 1.48 (s, 36H). $^{13}$C NMR (125 MHz, CD$_2$Cl$_2$): *δ* 175.73, 155.88, 155.71, 151.93, 150.70, 143.88, 143.60, 137.23, 134.53, 127.07, 125.88, 124.00, 123.64, 123.48, 122.20, 121.59, 121.36, 117.43, 116.15, 115.66, 111.63, 110.84, 34.06, 31.02. HRMS (*m/z*) calcd for $C_{42}H_{25}N_3O_2$ [M + Na]$^+$: 850.4348; found: 850.4351.

**9,9'-(4-(4-(4,6-Diphenyl-1,3,5-triazin-2-yl)phenyl)pyridine-2,6-diyl)bis(3,6-di-tert-butyl-9*H*-carbazole) (PytBuCz-TRZ)**: The synthetic procedure was analogous to that described for PytBuCz-XT. PytBuCz-TRZ was obtained as yellow solid in 73.7% yield. $^1$H NMR (500 MHz, CDCl$_3$): *δ* (ppm) 8.97 (d, *J* = 8.3 Hz, 2H), 8.83–8.77 (m, 4H), 8.16 (d, *J* = 1.8 Hz, 4H), 8.06 (d, *J* = 8.7 Hz, 4H), 7.99 (d, *J* = 8.4 Hz, 2H), 7.88 (s, 2H), 7.65–7.58 (m, 6H), 7.50 (m, 4H), 1.48 (s, 36 H); $^{13}$C NMR (125 MHz, CDCl$_3$): *δ* 171.97, 171.12, 152.70, 152.23, 144.44, 141.84, 138.11, 137.61, 136.26, 132.83, 130.06, 129.17, 128.86, 128.80, 127.63, 124.86, 124.25, 116.28, 111.92, 34.94, 32.09. HRMS (*m/z*) calcd for

$C_{66}H_{64}N_6$ $[M + Na]^+$: 941.5284; found: 941.5271.

## Additional spectra

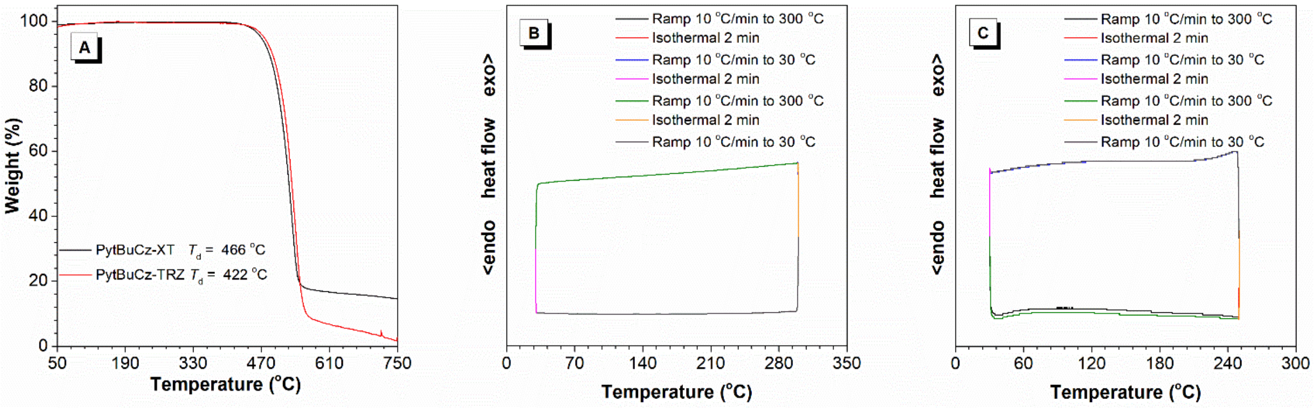

**Fig. S1** (A) TGA and DSC thermograms of B) PytBuCz-XT and C) PytBuCz-TRZ.

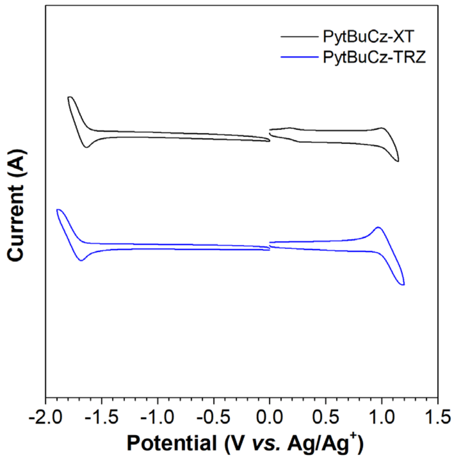

**Fig. S2** (A) Cyclic voltammograms of PytBuCz-XT and PytBuCz-TRZ.

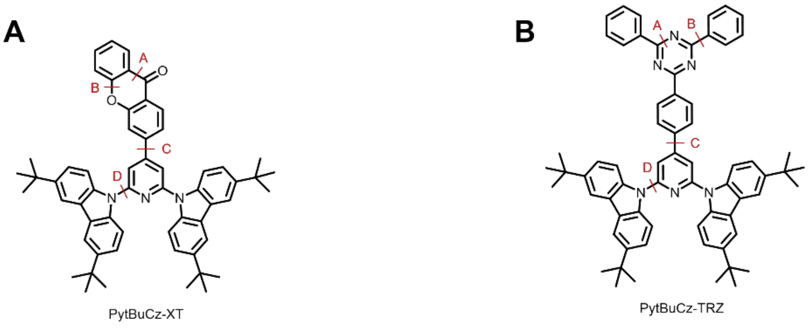

| | A | B | C | D |
|---|---|---|---|---|
| Neutral | 18.7 | 33.4 | 5.0 | 3.7 |
| Cation | - | - | 6.9 | 11.1 |
| Anion | - | - | 5.1 | 1.7 |

| | A | B | C | D |
|---|---|---|---|---|
| Neutral | 15.4 | 4.9 | 5.0 | 3.7 |
| Cation | - | 3.9 | 6.6 | 11.0 |
| Anion | - | 4.8 | 3.6 | 1.7 |

**Fig. S3** BDEs calculation results of A) PytBuCz-XT and B) PytBuCz-TRZ.

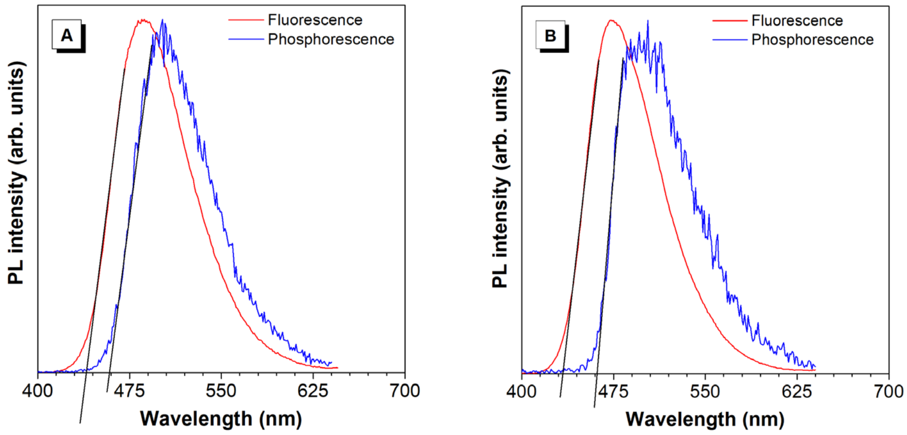

**Fig. S4** Fluorescence and phosphorescence spectra of the doped films in PPF host (15 wt%) of A) PytBuCz-XT and B) PytBuCz-TRZ, measured at 77 K.

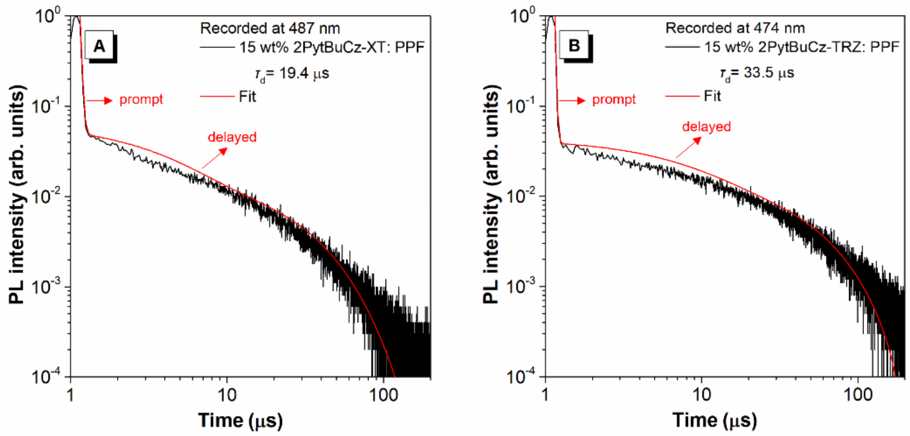

**Fig. S5** Transient decay spectra of the doped films of A) PytBuCz-XT and B) PytBuCz-TRZ, measured under nitrogen atmosphere.

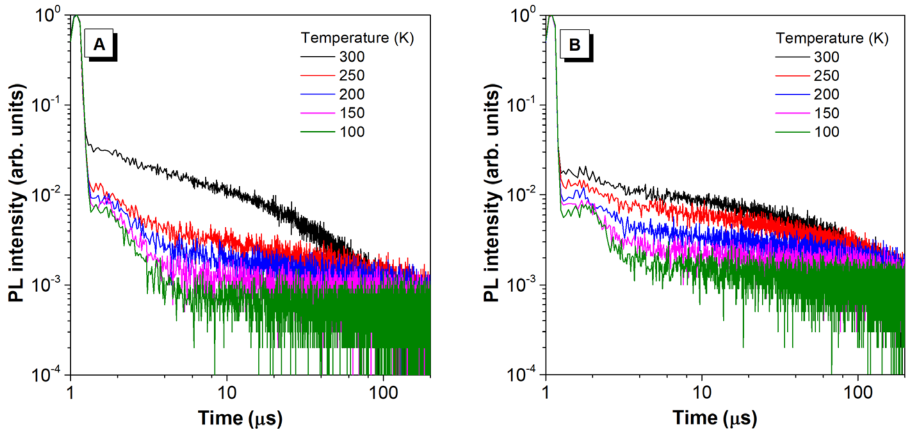

**Fig. S6** Temperature-dependent transient decay spectra of the neat films of A) PytBuCz-XT and B) PytBuCz-TRZ, measured at nitrogen atmosphere.

**Table S1**. The detailed data of temperature-dependent transient PL decay spectra of PytBuCz-XT and PytBuCz-TRZ in doped films.

| Compound | $T$ (K) | $<\tau>$ (μs) | $T_{\text{prompt}}$ (ns) | $\tau_{\text{delayed}}$ (ns) | $R_{\text{delayed}}$ (%) |
|---|---|---|---|---|---|
| PytBuCz-XT | 300 | 17.3 | 38 | 19468 | 88.8 |
| | 250 | 21.4 | 33 | 28190 | 75.9 |
| | 200 | 9.2 | 33 | 19378 | 47.2 |
| | 150 | 0.3 | 27 | 1154 | 21.4 |
| | 100 | 0.2 | 26 | 1133 | 19.7 |
| PytBuCz-TRZ | 300 | 29.3 | 52 | 33545 | 87.3 |
| | 250 | 38.9 | 51 | 46915 | 82.9 |
| | 200 | 20.4 | 46 | 27075 | 75.4 |
| | 150 | 4.1 | 28 | 1162 | 34.0 |
| | 100 | 2.1 | 26 | 709 | 26.3 |

**Table S2**. The detailed data of temperature-dependent transient PL decay spectra of PytBuCz-XT and PytBuCz-TRZ in neat films.

| Compound | $T$ (K) | $<\tau>$ (μs) | $T_{\text{prompt}}$ (ns) | $\tau_{\text{delayed}}$ (ns) | $R_{\text{delayed}}$ (%) |
|---|---|---|---|---|---|
| PytBuCz-XT | 300 | 23.9 | 26 | 32447 | 73.7 |
| | 250 | 21.2 | 29 | 43099 | 49.1 |
| | 200 | 12.9 | 30 | 37865 | 34.0 |
| | 150 | 1.4 | 28 | 1667 | 8.5 |
| | 100 | 0.8 | 29 | 1102 | 6.8 |
| PytBuCz-TRZ | 300 | 32.8 | 15 | 53030 | 61.8 |
| | 250 | 31.4 | 15 | 59383 | 52.8 |
| | 200 | 22.1 | 16 | 59110 | 37.3 |
| | 150 | 3.2 | 16 | 29300 | 10.8 |
| | 100 | 9.9 | 16 | 47404 | 20.8 |

## Reference

1 M. J. Frisch, G. W. Trucks, H. B. Schlegel, G. E. Scuseria, M. A. Robb, J. R. Cheeseman, G. Scalmani, V. Barone, B. Mennucci, G. A. Petersson, H. Nakatsuji, M. Caricato, X. Li, H. P. Hratchian, A. F. Izmaylov, J. Bloino, G. Zheng, J. L. Sonnenberg, M. Hada, M. Ehara, K. Toyota, R. Fukuda, J. Hasegawa, M. Ishida, T. Nakajima, Y. Honda, O. Kitao, H. Nakai, T. Vreven, J. J. A. Montgomery, J. E. Peralta, F. Ogliaro, M. J. Bearpark, J. Heyd, E. N. Brothers, K. N. Kudin, V. N. Staroverov, R. Kobayashi, K. R. J. Normand, A. P. Rendell, J. C. Burant, S. S. Iyengar, J. Tomasi, M. Cossi, N. Rega, N. J. Millam, M. Klene, J. E. Knox, J. B. Cross, V. Bakken, C. Adamo, J. Jaramillo, R. Gomperts, R. E. Stratmann, O. Yazyev, A. J. Austin, R. Cammi, C. Pomelli, J. W. Ochterski, R. L. Martin, K. Morokuma, V. G. Zakrzewski, G. A. Voth, P. Salvador, J. J. Dannenberg, S. Dapprich, A. D. Daniels, O. Farkas, J. B. Foresman, J. V. Ortiz, J. Cioslowski and D. J. Fox, Gaussian, *Inc*., Wallingford, *CT*, USA 2009.